CONF-8309137--3

INVERSE PLASMA EQUILIBRIA*

CONF-8309137--3

DE84 000723

H. R. Hicks**, R. A. Dory and J. A. Holmes**
Oak Ridge National Laboratory
Oak Ridge, Tennessee 37830 USA

ABSTRACT

In inverse equilibrium models, space variables (for example $\{R,Z,\zeta\}$) are determined as functions of magnetic variables $\{\rho,\Theta,\zeta\}$ using the usual MHD equations $\nabla \times \underline{B} = \mu_0 \underline{J}$, $\nabla \cdot \underline{B} = 0$, and $\underline{F} = \nabla p - \underline{J} \times \underline{B} = 0$. Analytical inverse models have long clarified the physics of both MHD equilibrium and stability [cf. Zakharov and Shafranov (1978)]. Inverse numerical models in two dimensions (2D) have led to a progression of increasingly sophisticated numerical codes [e.g., Potter (1976); Vabishchevich, et al., (1978,82); Takeda and Tsunematsu (1979); Delucia, Jardin and Todd (1980); Lao, Hirshman and Wieland (1981); Shumaker (1983); Ling (1983)]. In three dimensions, a similar progression of models has occurred [e.g., Bauer, Betancourt, and Garabedian (1978,1981); Schlüter and Schwenn (1981); Bhattacharjee, Wiley and Dewar (1982); Hirshman and Whitson (1983)]. These will be reviewed in this paper.

We illustrate in some detail a 2D inverse equilibrium solver that was constructed to analyze tokamak configurations and stellarators (the latter in the context of the average method). To ensure that the method is suitable not only to determine equilibria, but also to provide appropriately represented data for existing stability codes, it is important to be able to control the Jacobian, $\tilde{J} \equiv \partial(R,Z)/\partial(\rho,\Theta)$. The form chosen is $\tilde{J} = J_0(\rho)R^{\ell}\rho$ where ρ is a flux surface label, and ℓ is an integer. The initial implementation is for a fixed conducting wall boundary, but the technique can be extended to a free boundary model.

*Research sponsored by the Office of Fusion Energy, U.S. Department of Energy, under contract W-7405-eng-26 with the Union Carbide Corporation.

**Computer Sciences at ORNL.

1. Introduction

The calculation of equilibria has proved central to the study of laboratory plasmas. The existence and features of the equilibria are important for the design and understanding of confinement devices and experiments. Moreover, other calculations, such as particle orbits, transport, linear MHD stability, and nonlinear MHD evolution often require an equilibrium as a starting point. For most devices and calculations of interest, it is not a good approximation to assume that the equilibrium magnetic field (for a finite β plasma) is similar to the vacuum (zero β) field. Thus the equilibrium calculation provides a crucial link between the device design and these other calculations. Many approaches have been taken in this fertile field; we will focus on recent numerical work while providing some historical background.

Analytical plasma equilibrium calculations have been reviewed by Solev'ev and Shafranov [1]. For several cases, analytic solutions to the axisymmetric (tokamak) problem are known [2,3]. Numerical studies for (open-ended) magnetic mirror systems [4] were reported in the 1960's. For toroidal devices, numerical studies became common in the 1970's when complicated configurations with no evident expansion parameters were analyzed; typical examples are provided by Refs. [5-10]. In these approaches the solution is expressed in a predefined fixed coordinate system, so we will refer to them as Eulerian methods. Eulerian methods may use geometric (e. g. Cartesian or cylindrical) coordinates or coordinates suggested by the boundary or by a vacuum field. In the axisymmetric case, one obtains the poloidal magnetic flux, ψ, as a function of space coordinates; for example

$\psi(R,Z)$, where R is the major radius and $\{R,Z,\zeta\}$ defines a cylindrical coordinate system. One can also use global basis functions in one or more dimensions. The required form of the solution dictates whether a finite difference grid, a set of finite elements, or a set of global basis functions provides the most economical and concise representation. To cite two examples, Eulerian methods in three dimensions have been implemented on a 3D grid [11] and with a mixed representation in vacuum flux coordinates using 2D global angle functions (Fourier expansions) and a 1-D flux surface grid [12].

For stability studies, $\psi(\rho)$ and the "inverse functions" $R(\rho,\Theta)$, and $Z(\rho,\Theta)$ are frequently required to define the equilibrium. Here, Θ is a generalized poloidal angle and ρ is a flux surface label. Obtaining these functions from $\psi(R,Z)$ by integrating along flux contours (as one would do in an Eulerian method) can involve significant truncation error-especially near a magnetic axis which does not coincide with an axis of the predefined coordinate system.

Inverse methods are designed to determine (usually iteratively) the inverse functions directly in terms of the $\{\rho,\Theta\}$ coordinate system. As in Eulerian methods, functions of (ρ,Θ) can be represented in several ways: on a finite difference grid, as a set of finite elements, with a set of global basis functions, or as some combination of these. A key advantage of inverse methods is that they can provide more accurate input for stability calculations. They also (generally) constrain the flux topology. For 2D calculations, existence of solutions with toroidal topology can be guaranteed [13]. However, for 3D solutions, no general existence proof is known and therefore

numerical solutions obtained with the inverse method and forced to obey the topology constraints are not guaranteed to converge uniformly to a true solution of the equations. For example, equilibria containing separatrices or ergodic regions will not be found with inverse method codes unless provision is made to treat multiple regions and to match solutions where these regions meet.

In inverse analyses, the spatial coordinates $\{R,Z\}$ are determined as functions of magnetic variables $\{\rho,\Theta,\zeta\}$, where ρ labels 'magnetic' surfaces of constant ψ on which plasma pressure is uniform and in which magnetic field lines are constrained to lie. The independent coordinates Θ and ζ are frequently taken to be angular in nature since the ψ surfaces are toroids. Generally, the $\{\rho,\Theta,\zeta\}$ system is nonorthogonal.

Our attention here will be restricted to inverse equilibrium calculations for toroidal systems with isotropic pressure, zero flow, and magnetic surfaces having rotational transform. Such systems include tokamaks, stellarators and reversed field pinch devices. While magnetic mirror and bumpy torus equilibrium analyses share many of the same features, the necessary generalizations would make this review cumbersome.

The work of Shafranov [14], and of Johnson, Greene and Weimer [14] provides early analytical application of the inverse method in the calculation of the relative shift of magnetic surfaces in stellarators and tokamaks as plasma pressure rises from zero. In these studies, only a small number (1-5) of parameters is used to represent the equilibrium fields, and increasing this number in order to provide

arbitrarily high accuracy appears prohibitive. A more recent example has been given by V. D. Khait [15] in which the parameters are the relative shift and the ellipse ratio (logarithm of ratio of major to minor axis). Solution is accomplished by the use of a variational method. Related discussions appear in references [16] and [17]. Proceedings of the U.S.-Japan workshops on 3D MHD [18,19] also include papers on recent work in those two countries.

1.1 Inverse Numerical Methods in Two Dimensions

An early attempt to generalize the inverse method to arbitrarily high accuracy was that of D. Potter [20] in the article called "Waterbag Methods in MHD." The term 'waterbag' derived from earlier calculations [21,22] of one dimensional Vlasov models where the area enclosed by contours of fixed phase space density (i. e., waterbags) is preserved by the dynamics. Potter, using special orthogonal coordinates, applied a variational method akin to 'steepest descent' to relax in two dimensions the position of the magnetic surfaces for a tokamak equilibrium, the preserved quantities here being magnetic fluxes.

Zakharov and Shafranov [23] discuss 2D equilibria (static and evolutional) from both analytic and numerical points of view. They pose the problem on an orthogonal 2D inverse grid. Solutions are obtained for fixed boundary cylindrical cases. They comment that the inverse method may be the method of choice over the traditional Eulerian approach, even for multiply connected regions. However, they anticipate technical difficulties with the inverse method in toroidal

cases because of the difficulty of determining the position of the magnetic axis.

Vabishchevich, et al. [24] formulate a fully numerical inverse equilibrium procedure in two dimensions. Orthogonal independent coordinates ψ, θ are used as a representation for the unknown cylindrical coordinate functions R, Z of the magnetic surface. The coupled elliptic partial differential equations are then solved on a grid in $\{\psi,\theta\}$ space by numerical methods not detailed in the paper. Fixed and free boundary solutions are obtained both for cylinders and finite aspect ratio toroids.

Takeda and Tsunematsu [19,25] apply finite element methods using a set of equally spaced nodes on the magnetic surfaces to determine axisymmetric, fixed boundary, tokamak equilibria. An inner iteration solves the nonlinear eigenvalue problem; and in an outer iteration, surfaces are determined by tracing lines of constant ψ in the coordinates of the previous step. The authors provide [25] sample data and output as well as a partial listing and a detailed description of the iteration procedure used in their code SELENE.

Delucia, Jardin and Todd [26] also employ a 2D flux coordinate grid, but they explicitly constrain the Jacobian and they pose the problem in finite difference form. They include discussion of the free boundary problem and also the option of constraining the rotational transform. Their description [26] is detailed and includes flowcharts of the iteration process.

Shumaker [27] obtains 2D equilibria of compact torus configurations for transport studies. He has developed a fast finite element inverse code which is able to handle configurations having a separatrix. Rather than a Jacobian or orthogonality constraint, he locates nodes where needed for accuracy. He constrains two adiabatic quantities rather than $F(\psi)$ and $P(\psi)$. His solution is obtained with an ICCG (Incomplete Cholesky Conjugate Gradient) technique. This is the only inverse code we are aware of which treats a nonsimple topology.

An inverse method for tokamak equilibria in two dimensions has been developed, using a moments representation, by Lao and co-workers [28-30]. This has been fully documented in a technical report [30] including a microfiche of the actual coding. This code (VMOMS) uses a shooting method to solve for the Fourier amplitudes (moments) in polar angle θ as function of a radial or flux coordinate ρ. The code uses a 'fixed boundary' treatment in which the outermost magnetic surface is prescribed in space. The properties of this code include a high degree of efficiency, and a good representation using a modest number of parameters, typically $\lesssim 5$ Fourier coefficients on each of $\simeq$ 20-30 magnetic surfaces. This code was developed to treat the moderate resolution cases that are needed in transport simulation studies. For potential applications requiring high precision, such as some stability analyses, the code may not react well to substantial increases in the number of harmonics or the number of surfaces used.

Pustovitov, et al. [31] reports numerical results for 2D equilibria using the stellarator expansion [32]. The inverse method

used here is an iteration on a finite difference grid, which is described in earlier papers by Vabishchevich [33].

Ling [34] has developed a code which uses the method of Lao [28-30] for the fixed boundary problem. Free boundary calculations can also be done with this code, including ones in which the plasma moves through a series of quasi-static free boundary equilibria consistent with currents in external coils.

We are developing an alternate approach, which allows control of the Jacobian. In later sections of this paper, we describe such a code (AXE) having several important distinctions brought about by its intended application: to provide high resolution equilibrium data for stability analysis of tokamaks, and for applying the average method approach to the study of stellarator systems [14,32]. Important to reducing numerical 'pollution' of the mode spectra for such stability analysis is that the Jacobian $\tilde{J} \equiv \partial(R,Z)/\partial(\rho,\Theta)$ take the form $J_0(\rho)R^{\ell}\rho$ where the particular choice $\ell = 2$ leads to natural magnetic coordinates where field lines are straight, having the form $\Theta - t\zeta = \text{constant}$. This code uses Fourier decomposition in angle Θ, and a prescribed (fixed) outermost magnetic surface boundary condition.

1.2 Inverse Methods in Three Dimensions

The problem of equilibrium in a stellarator or in a real tokamak with symmetry-spoiling elements such as finite toroidal field coils or bundle divertors may require a fully three dimensional treatment. Eulerian codes [11,12] have been important in the analysis of systems

with complex magnetic topology, but the limited resolution available with present computers makes 3D inverse method codes desirable as well.

An early implementation which is still in widespread use was devised by Bauer, Betancourt, and Garabedian [18,19,35] who also provide references to earlier work. This code uses magnetic coordinates, a 3D finite difference grid, an energy principle, and an accelerated steepest descent method to generate equilibria. A vacuum region surrounding the plasma is permitted and at the free boundary between plasma and vacuum, the continuity of $B^2/2\mu_0 + P$ is maintained. A version of the code is listed in Reference 35 and the method is extensively described. More recently, Schlüter and Schwenn [36] have developed a similar code (TUBE) which differs primarily in the details of the iteration scheme.

Extension of the moments method [28-30] to three dimensions was considered by Bhattacharjee [18] who wrote out moment equations based on a Lagrangian formulation, and later, with Wiley and Dewar [37], presented equilibria in three dimensions using the geometrical toroidal angle as the choice for ζ in the magnetic representation.

Two important advances have been proposed by Hirshman and Whitson [38] who observed that the enlightened choice of angle variables $\{\theta,\zeta\}$ (as in [28,29]) would enhance convergence of the Fourier series, and that using an adiabatic energy principle with index $\gamma > 1$ ensures a nonnegative quadratic form, leading to monotonic convergence of the steepest descent iterative solution. An energy principle is used in this method to generate the transformation ('renormalization') between the straight field line coordinates and those variables which economize

the Fourier representation. Parenthetically, representation in the economizing variables should yield the most reliable identification between coefficients in "simple physical models" (surface shift, elongation, triangularity, etc.) and the results of the complete calculation.

2. A 2-D Inverse Equilibrium Code, AXE

We were motivated to develop an inverse equilibrium code, AXE (AXisymmetric Equilibrium), by our need for accurate 2D equilibria represented in terms of a (non-orthogonal) straight field line flux coordinate system $\{\rho,\Theta\}$. The inverse functions are required in the form of discrete representations in ρ and series expansions in Θ:

$$R(\rho,\Theta) = \sum_m R_m(\rho_j)\cos(m\Theta) \quad , \tag{2.1a}$$

and

$$Z(\rho,\Theta) = \sum_m Z_m(\rho_j)\sin(m\Theta) \quad , \tag{2.1b}$$

where ρ_j are a set of grid points. These requirements are dictated by our intended use for AXE to provide input for stability calculations [39] which assume this representation. Previously, we have obtained equilibria in other representations and then transformed to the one described above, but this compromises the accuracy somewhat. The new code can also serve as an accurate general-purpose equilibrium code. Since the stability calculations are, themselves, time consuming to carry out, the speed of AXE has been regarded as less important than its accuracy.

In addition to solving the usual equilibrium equation for Tokamak cases, we have designed AXE to allow it to be generalized to treat the Stellarator expansion model [14,32]. The code is intended to calculate noncircular, fixed boundary, arbitrary aspect ratio, 2D equilibria. AXE allows equilibria which are not symmetric across the toroidal

equator (i.e. not up/down symmetric). However, to simplify the discussion here, we will only outline the symmetric case. The asymmetric case is a simple, though tedious, generalization.

Using the stellarator expansion, the equilibrium equation becomes

$$\Delta^*\psi = - R^2P' - (F + F^*)F' + \Delta^*\psi_{vac}, \tag{2.2}$$

where

$$\Delta^*\psi \equiv R\frac{\partial}{\partial R}\left(\frac{1}{R}\frac{\partial}{\partial R}\psi\right) + \frac{\partial^2}{\partial Z^2}\psi, \tag{2.3}$$

$$P' \equiv \frac{\partial P(\psi)}{\partial \psi}, \quad F' \equiv \frac{\partial F(\psi)}{\partial \psi}, \quad F(\psi) \equiv RB_\zeta, \tag{2.4}$$

and where $F^*(R,Z)$ and $\Delta^*\psi_{vac}(R,Z)$ are obtained from the stellarator vacuum field [32]. This reverts to the normal tokamak case simply by taking F^*, $\psi_{vac} \to 0$

The Jacobian is given by requiring $RdRdZ = \tilde{J}d\rho d\Theta$. This gives

$$\tilde{J} \equiv (\nabla\rho \times \nabla\Theta \cdot \nabla\zeta)^{-1} = R\left(\frac{\partial R}{\partial \rho}\frac{\partial Z}{\partial \Theta} - \frac{\partial R}{\partial \Theta}\frac{\partial Z}{\partial \rho}\right). \tag{2.5}$$

We impose the constraint $\tilde{J} = J_0(\rho)\, R^\ell \rho$. The value $\ell = 2$ corresponds to the straight field line coordinate system which is needed for our stability codes, but we shall not restrict the value of ℓ at this point.

The toroidal angle ς is ignorable and orthogonal to both ρ and Θ. The general form for $\Delta^*\psi$ is

$$\Delta^*\psi = \frac{R^2}{J}\left[\frac{\partial}{\partial\rho}\left(h^{\rho\rho}\frac{\partial\psi}{\partial\rho}\right) + \frac{\partial}{\partial\Theta}h^{\rho\Theta}\frac{\partial\psi}{\partial\rho}\right]. \tag{2.6a}$$

where

$$h^{\rho\rho} = \left[\left(\frac{\partial R}{\partial\theta}\right)^2 + \left(\frac{\partial Z}{\partial\theta}\right)^2\right]/\tilde{J} \tag{2.6b}$$

and

$$h^{\rho\Theta} = -\left(\frac{\partial R}{\partial\Theta}\frac{\partial R}{\partial\rho} + \frac{\partial Z}{\partial\Theta}\frac{\partial Z}{\partial\rho}\right)/\tilde{J} \tag{2.6c}$$

Finally the nonlinear equations to be solved are

$$J_0(\rho)R^{\ell} = R\left(\frac{\partial R}{\partial\rho}\frac{1}{\rho}\frac{\partial Z}{\partial\Theta} - \frac{1}{\rho}\frac{\partial R}{\partial\Theta}\frac{\partial Z}{\partial\rho}\right) \tag{2.7}$$

and

$$\frac{R^{2(1-\ell)}}{J_0^2}\left\{J_0\rho\frac{\partial}{\partial\rho}\left(\frac{1}{J_0 r}\frac{\partial\psi}{\partial\rho}\right)\left[\frac{1}{\rho^2}\left(\frac{\partial R}{\partial\Theta}\right)^2 + \frac{1}{\rho^2}\left(\frac{\partial Z}{\partial\Theta}\right)^2\right]\right.$$

$$+\frac{\partial\psi}{\partial\rho}\left[\frac{1}{\rho}\frac{\partial R}{\partial\Theta}\frac{1}{\rho}\frac{\partial^2 R}{\partial\Theta\partial\rho} + \frac{1}{\rho}\frac{\partial Z}{\partial\Theta}\frac{1}{\rho}\frac{\partial^2 Z}{\partial\Theta\partial\rho} - \frac{1}{\rho^2}\frac{\partial^2 R}{\partial\Theta^2}\frac{\partial R}{\partial\rho}\right.$$

$$-\frac{1}{\rho^2}\frac{\partial^2 Z}{\partial\Theta^2}\frac{\partial Z}{\partial\rho} - \ell J_0 \frac{1}{\rho}\frac{\partial Z}{\partial\Theta} R^{\ell-2}\Big]\Big\} + R^2P' + (F + F^*)F' + \Delta^*\psi_{vac} = 0. \quad (2.8)$$

The quantities F, P, and ρ are taken as flux functions. Therefore, on the finite difference grid one can define in addition to Eq. (2.1)] $F(\rho_j)$, $\Psi(\rho_j)$, and $P(\rho_j)$. The boundary conditions at the magnetic axis ($\rho = 0$) are

$$\frac{\partial F}{\partial\rho} = \frac{\partial\psi}{\partial\rho} = \frac{\partial P}{\partial\rho} = \frac{\partial R_o}{\partial\rho} = 0 \quad (2.9a)$$

and

$$R_m = Z_m = 0 \text{ for } m \neq 0. \quad (2.9b)$$

At the wall ($\rho = 1$) one has

$$\psi = P = 0 \quad , \quad (2.9c)$$

and R_m, Z_m must approximate the desired boundary shape.

We choose to specify the safety factor $q(\rho)$. Using

$$q(\rho) = -\frac{J_o(\rho)\rho\, F(\rho)}{\frac{\partial\psi}{\partial\rho}} \langle R^{\ell-2}\rangle_{m=0} \quad . \quad (2.10).$$

where $\langle a\rangle_{m=0}$ is the m = 0 projection of a, one can relate $F(\rho)$, $J_o(\rho)$, and $\partial\psi/\partial\rho$. The pressure is taken as a power of ψ:

$$P(\psi) \equiv P_o \, (\psi/\psi_o)^i \, , \qquad (2.11)$$

where ψ_o is the axis value of ψ and P_0 is related to the central β by $\beta_0 F_0^2 = 2P_0 R_0^2$. Hereafter, we will consider the case i = 2.

The procedure used in AXE for solving Eqs. 2.7-2.11 is outlined in Fig. 1. The desired boundary is described by a sequence of points. Then the initial wall values of the coordinates R_m, Z_m, are determined by fitting these points with the assumption of some Θ along the surface curve. Next, a guess for the magnetic axis position, R_{ov}, is used to fix the initial coordinate axis. In the case of the Stellarator expansion technique, this could be the vacuum field axis position. A set of grid points in the coordinate ρ is chosen: $0 \leq \rho_j < 1$. Finally, the initial set of coordinates $R_{m,j}$ and $Z_{m,j}$ are fixed by interpolating between the wall values and R_{ov} using the points ρ_j. This completes the specification of the (somewhat arbitrary) initial coordinate system.

Next, we use the Jacobian equation (2.7) to modify the Θ coordinate, keeping the ρ-surfaces fixed. This is accomplished by moving, in small steps, tangential to constant-ρ surfaces. Such motion is described by

$$\tilde{R} = R_\Theta \, \tilde{\Theta} \text{ and } \tilde{Z} = Z_\Theta \, \tilde{\Theta} \qquad (2.12)$$

where the tilde indicates the increment due to the current iteration, e.g., $R^{k+1} = R^k + \tilde{R}$. Using these relations to linearize Eq. (2.7), we solve

$$-\frac{1}{\rho}\frac{\partial(\rho\tilde{\Theta})}{\partial\Theta}\left(\frac{R_\rho Z_\Theta - R_\Theta Z_\rho}{\rho}\right) - (\rho\tilde{\Theta})\frac{1}{\rho}\frac{\partial}{\partial\theta}\left[-J_0(\rho)R^{\ell-1} + \frac{R_\rho Z_\Theta - R_\Theta Z_\rho}{\rho}\right]$$

$$= -J_0(\rho)R^{\ell-1} = \frac{R_\rho Z_\Theta - R_\Theta Z_\rho}{\rho} \qquad (2.13)$$

for $\rho\tilde{\Theta}$. The $\rho\tilde{\Theta}$ term is of higher order than the other and can be omitted. For the up-down symetric case, one should require that $\tilde{\Theta} = 0$ at $\Theta = 0,\pi$. Thus, a suitable expansion for $\tilde{\Theta}$ is

$$\tilde{\Theta} = \sum_{m>0} \tilde{\Theta}^m \sin m\theta \quad . \qquad (2.14)$$

If the series in 2.1 and 2.14 are terminated at $m = M$, then there is one more equation (2.13) than unknown (2.15). This is because the $m = 0$ projection of Eq. (2.7) determines the ρ-dependence of the Jacobian:

$$J_o(\rho) \equiv \frac{\left\langle \frac{R_\rho Z_\Theta - R_\Theta Z_\rho}{\rho} \right\rangle_{m=0}}{\langle R^{\ell-1}\rangle_{m=0}} \quad . \qquad (2.15)$$

So, given the initial (or previous) coordinates, R_m and Z_m, we solve (2.15) for $J_0(\rho)$. The coupled set of Eqs. (2.13) is then solved for $\tilde{\Theta}_m$ at each j. In practice, the right hand side of Eq. (2.13) is multiplied by a factor λ_1 [shown in Eq. (3.1)] so that $\tilde{\Theta}$ is limited in size. If it were too large, the tangent condition (2.12) would allow the ρ-surfaces to move visably outward.

Now, using the new coordinates

$$R^{k+1} = R^k + R_\Theta \tilde{\Theta} \ , \tag{2.16a}$$

and

$$Z^{k+1} = Z^k + Z_\Theta \tilde{\Theta} \ , \tag{2.16b}$$

one repeats this procedure until $\tilde{\Theta}$ is sufficiently small. Figure 2 shows the maximum (in space) values of $\tilde{\Theta}$ as a function of iteration number for three different values of M. The value of M necessary for convergence will depend on the configuration, and will not always lie between 8 and 13 as it does here. The convergence is very rapid, with $\tilde{\Theta}_{max}$ dropping an order of magnitude every few steps. During this iteration we recalculate $J_0(\rho)$ using Eq. (2.15) on each iteration. However, the tangent condition (2.12) insures that it will be essentially unchanged. The Θ derivatives are performed analytically and the ρ derivatives are performed with 3-point finite difference formulae. These equations involve convolutions either explicitly [as in (2.13), (2.15), and (2.16)] or implicitly as [as in Eq. (2.13)]. To do this, we construct matrices, $C_{m,m',m''}$, whose elements contain the contribution to a component m for component m' multiplied by component m''. There are three such matrices to account for the possibilities of convoluting a cosine series with a sine series, a cosine series with a cosine series, or a sine series with a sine series. We use routine F04ARF from the Numerical Algorithms Group (NAG) Library [41] to solve

the system of simultaneous Eqs. (3.1) for $\tilde{\Theta}_m$, but this choice is not essential.

Having solved the Jacobian equation, the equilibrium equation (2.8) is solved by keeping the constant-Θ contours fixed and moving the ρ contours. This time we use the tangent conditions

$$\tilde{R} = R_\rho \tilde{\rho} \text{ and } \tilde{Z} = Z_\rho \tilde{\rho} , \tag{2.17}$$

with $\tilde{\rho}$ expanded as

$$\tilde{\rho} = \sum_m \tilde{\rho}_m \cos m\Theta. \tag{2.18}$$

If we were to allow $\tilde{\rho}_0 \neq 0$, then the boundary conditions would not be satisfied, so instead we solve for $\psi(\rho)$ and $\tilde{\rho}_m (m > 0)$. Eliminating P in Eq. (2.8) with Eq. (2.11) and eliminating F with (2.10), one obtains by projecting out the $m = 0$ component, an equation for ψ of the form

$$D_2 \frac{\partial^2 \psi}{\partial \rho^2} + D_1 \frac{\partial \psi}{\partial \rho} + D_0 \frac{\psi}{\psi_o} = 0. \tag{2.19}$$

The coefficients are specified in Eq. (3.2). Using the origin boundary condition $\partial\psi/\partial\rho = 0$, and the wall condition, $\psi = 0$, it is necessary to iterate (2.19) to arrive at the origin value ψ_o. This iteration also proceeds rapidly and normally converges in fewer than 10 steps.

Finally, we observe that the force in the ρ direction, given by $(\vec{J} \times \vec{B})_\rho - \partial_\rho p$ can be obtained by multiplying Eq. (2.8) by $-R^{-2}\partial\psi/\partial\rho$. Taking only the $m \neq 0$ projections of the force we set

$$\tilde{\rho}_m = \lambda_2\left[(\tilde{J} \times \tilde{B})_\rho - \partial_\rho P\right]_m . \tag{2.20}$$

As with $\tilde{\Theta}_m$, it is necessary to restrict the magnitude of $\tilde{\rho}_m$ (using λ_2) so that the tangent condition does not move the constant-Θ lines.

Once the coordinates are updated using Eq. (2.17), it is necessary to return to the Jacobian equation. This overall iteration is illustrated in Fig. 1.

With the equations in this form, one can include the Stellarator expansion terms F^* and $\Delta^*\psi_{vac}$, which are defined in $\{R,Z\}$ coordinates, by projecting them into the current coordiantes whenever they are needed, e.g.,

$$F^*_m(\rho) \equiv \frac{1}{2\pi}\int_0^{2\pi} F^*(R,Z)\Big|_\rho \cos m\Theta \, d\Theta. \tag{2.21}$$

If they are stored on a vacuum flux grid or a polar grid, the integral can be performed accurately.

3. Equations Solved in AXE

In this section, we summarize the equations solved in AXE. Using the techniques described in Section 2, AXE iteratively solves

$$-\frac{\partial\tilde{\Theta}}{\partial\Theta}\left(\frac{R_\rho Z_{A\Theta}-R_\Theta Z_\rho}{\rho}\right)=\lambda_1\left[-J_0(\rho)R^{\ell-1}+\frac{R_\rho Z_\Theta-R_\Theta Z_\rho}{\rho}\right], \tag{3.1}$$

using Eqs. (2.14) and (2.15), and the previous values for R and Z. The resulting $\tilde{\Theta}$ is used in Eq. (2.12). Next, $\psi(\rho)$ is obtained by solving Eq. (2.19) where

$$D_2=\langle R_\Theta^2+Z_\Theta^2+q^2R^{2(\ell-1)}\rangle_{m=0} \tag{3.2a}$$

$$D_1=\langle J_0\rho q\frac{\partial}{\partial\rho}\left(\frac{q}{\rho J_0}\right)R^{2(\ell-1)}$$

$$+R_\Theta R_{\Theta\rho}+Z_\Theta Z_{\Theta\rho}-R_{\Theta\Theta}R_\rho-Z_{\Theta\Theta}Z_\rho-\ell J_0\rho Z_\Theta R^{\ell-2}\rangle_{m=0} \tag{3.2b}$$

$$D_0=\langle 2P_0\rho^2J_0^2R^{2\ell}\rangle_{m=0}. \tag{3.2c}$$

Finally, one obtains $\tilde{\rho}$ with

$$\tilde{\rho}=\lambda_2\frac{\partial\psi}{\partial\rho}\frac{1}{R^2}\left\{\frac{R^{2(1-\ell)}}{J_0^2}\left[J_0\rho\frac{\partial}{\partial\rho}\left(\frac{1}{J_0\rho}\frac{\partial\psi}{\partial\rho}\right)\left[\frac{1}{\rho^2}(R_\Theta^2+Z_\Theta^2)\right]\right.\right.$$

$$\left.+\frac{\partial\psi}{\partial\rho}\left(\frac{1}{\rho^2}R_\Theta R_{\Theta\rho}+\frac{1}{\rho^2}Z_\Theta Z_{\Theta\rho}-\frac{1}{\rho^2}R_{\Theta\Theta}R_\rho-\frac{1}{\rho^2}Z_{\Theta\Theta}Z_\rho-\ell J_0\frac{1}{\rho}Z_\Theta R^{\ell-2}\right)\right]$$

$$\left.+R^2P'+FF'\right\}, \tag{3.3}$$

for use in Eq. (2.17). With this updated coordinate system, one goes back to solve Eq. (3.1), as indicated in Fig. 1.

References

[1] L. S. Solov'ev and V. D. Shafranov in "Reviews of PLasma Physics, Vol. 5" Consultants Bureau, New York 1970; V. D. Shafranov, Phys. Fluids 26 (1983) 357.

[2] V. D. Shafranov, "Reviews of Plasma Physics" Vol. 2, p. 103, Consultants Bureau, New York 1966; F. Hernegger, Fifth European Conf. on Controlled Fusion and Plasma Physics (Euratom CEA, Grenoble, 1972), Vol. I, p. 26; E. K. Maschke, Plas. Physics 15 (1973) 535; J. P. Sudano, Phys. Fluids 17 (1974) 1915; E. Mazzucato, Phys. Fluids 18 (1975) 536; C. S. Lai, Mary Verleun, Phys. Fluids 19 (1975) 1066.

[3] L. S. Solov'ev, Soviet Physics JETP 26 (1968) 400 [Zh. Eksp. Teor. Fiz. 53 (1967) 626]

[4] J. Killeen and K. Whiteman, Phys. Flu. 9 (1966) 1846.

[5] J. D. Callen and R. A. Dory, Phys. Flu. 15 (1972) 1523;

[6] A. E. Bazhanova and V. D. Shafranov, Sov. Phys. Tech. Phys. 16 (1972) 1068.

[7] K. Lackner, Computer Phys. Communications 12 (1976) 33.

[8] J. L. Johnson et al., J. Comp. Phys. 32 (1979) 212.

[9] D. B. Nelson and C. L. Hedrick, Nucl. Fus. 19 (1979) 283.

[10] J. A. Holmes, Y-K. M. Peng and S. J. Lynch, J. Comp. Phys. 36 (1980) 35.

[11] R. Chodura, A. Schlüter, J. Comp. Phys. 41 (1981) 68; L. Garcia, B. A. Carreras, J. H. Harris, H. R. Hicks, and V. E. Lynch, "Equilibrium Studies for Low Aspect Ratio Torsatrons," Oak Ridge National Laboratory Report ORNL/TM-8833 (to be pub.).

[12] T. C. Hender, B. A. Carreras, L. Garcia, V. E. Lynch, H. R. Hicks, J. A. Holmes, B. F. Masden and J. A. Rome, "Torsatron Equilibria in Vacuum Flux Coordinates," (to be pub.).

[13] M. D. Kruskal and R. M. Kulsrud, Phys. Fluids 1 (1958) 265.

[14] V. D. Shafranov, Nucl. Fus. 8 (1968) 253; and J. M. Greene, J. L. Johnson, and K. E. Weimer, Phys. Flu. 14 (1971) 671.

[15] V. D. Khait, Sov. J. Plasma Physics 6 (1980) 476; V. D. Khait and V. K. Kolesnikov, 10th European Conf., Moscow, 1981.

[16] V. D. Pustovitov, Sov. J. Plas. Phys. 8 (1982) 265.

[17] M. I. Mikhailov and V. D. Shafranov, XIth European Conf. on Controlled Fus. and Plasma Physics, Aachen (1983).

[18] Proceedings of the U.S.-Japan Workshop on 3D MHD Studies for Toroidal Devices, Oak Ridge TN, Oct. 19-21,1981, B. A. Carreras, Editor, Oak Ridge National Laboratory Report ORNL-Conf-81/10101 (1982).

[19] Proceedings of the U.S. Japan Workshop on 3D MHD Simulation, Nagoya, Japan, March 7-11, 1983, Tetsuya Sato, Editor, Nagoya University Institute of Plasma Physics Report IPPJ-632 (1983).

[20] D. Potter, Methods in Computational Physics 16 (1976) 43.

[21] D. C. DePakh, J. Electron. Contr. 10 (1962) 417.

[22] R. A. Dory, J. Nucl. Energy C6 (1964) 511.

[23] L. E. Zakharov and V. D. Shafranov, Kurchatov Inst. Report IAE-3075 (1978). ["Problems in the Evolution of Equilibria of Toroidal Configurations", Oak Ridge National Laboratory Translation ORNL/TR-4667].

[24] P. N. Vabishchevich, L. M. Degtyarëv and A. P. Favorskii, Fiz. Plasmy 4 (1978) 995 [Sov. Journ. Plasma Physics, 4 (1978) 554].

[25] T. Takeda and T. Tsunematsu, "A Numerical Code SELENE to Calculate Axisymmetric Toroidal MHD Equilibria", Japan Atomic Energy Research Inst. Report JAERI-M 8042 (1979).

[26] J. Delucia, S. C. Jardin and A. M. M. Todd, J. Comp. Phys. 37 (1980) 183.

[27] D. E. Shumaker, "Numerical Calculation of Compact Torus Equilibrium", Lawrence Livermore National Laboratory, Report UCRL-88535 (1983).

[28] L. L. Lao, S. P. Hirshman and R. M. Wieland, Phys. Fluids 24 (1981) 1431.

[29] L. L. Lao, R. M. Wieland, W. A. Houlberg and S. P. Hirshman, Comp. Phys. Comm. 27 (1982) 129.

[30] L. L. Lao, R. M. Wieland, W. A. Houlberg and S. P. Hirshman, "VMOMS-A Computer Code for Finding Moment Solutions to the Grad-Shafranov Equation", Oak Ridge National Laboratory Report ORNL/TM-7871 (1982).

[31] V. D. Pustovitov, V. D. Shafranov, L. E. Zakharov, L. M. Degtyarev, V. V. Drozdov, S. Yu. Medvedev, Yu. Yu. Poshekhonov, M. I. Mikhajlov, "Computation of Plasma Equilibrium and Stability in Stellarators on the Basis of a Generalized Two-dimensional Equilibrium Equation", in Plasma Physics and Controlled Nuclear Fusion Research (Proceedings 9th Int. Conf., Baltimore, 1972), Vol. 2, IAEA, Vienna (1983) 541.

[32] J. M. Greene, J. L. Johnson, Phys. Fluids 4 (1961) 875; L. M. Kovrizhnykh and S. V. Shchepetov, Sov. J. Plas. Physics 6 (1980) 533; L. M. Kovrizhnykh and S. V. Shchepetov, Preprint No. 36,

P. N. Lebedev Physic Institute, Academy of Sciences of the USSR, Moscow (1980); V. D. Pustovitov, Nuclear Fusion 23 (1983) 1079.

[33] P. N. Vabishchevich, L. M. Degtyarev, V. V. Drozdov, I.P.M. Acad. Sci. Preprint #112 (1981); P. N. Vabishchevich, L. M. Degtyarev, V. V. Drozdov, Dokl. Akad. Nauk SSSR 262 (1982) 1040 [Soviet Math. Dokl. 25 (1982) 153].

[34] K. M. Ling, et al., "The Princeton Spectral Equilibrium Code: PSEC", Princeton Plasma Physics Laboratory Report PPPL-2029 (1983); Private communication.

[35] F. Bauer, O. Betancourt and P. Garabedian "A Computation Method in Plasma Physics," (Springer-Verlag, NY, 1978); F. Bauer, O. Betancourt and P. Garabedian, Phys. Fluids 24 (1981) 48.

[36] A. Schlüter and U. Schwenn, Comp. Phys. Comm. 24 (1981) 263.

[37] A. Bhattacharjee, J. C. Wiley and R. L. Dewar, "Variational Method for the Three-Dimensional Inverse Equilibrium Problem in Toroids" University of Texas, Austin, Institute for Fusion Studies Report IFSR 48-R (1983).

[38] S. P. Hirshman, and J. C. Whitson, "Steepest Descent Moment Method for Three Dimensional Magnetohydrodynamic Equilibria" Phys. Fluids (to be published); S. P. Hirshman and J. C. Whitson, Proc. 1983 Sherwood Theory Meeting, March 1983, Arlington, VA.

[39] H. R. Hicks, B. Carreras, J. A. Holmes, D. K. Lee and B. V. Waddell, J. Comp. Phys. 44 (1981) 46; V. E. Lynch, B. A. Carreras, H. R. Hicks, J. A. Holmes, and L. Garcia, Computer Phys. Communications 24 (1981) 465; B. A. Carreras, H. R. Hicks,

J. A. Holmes, V. E. Lynch, L. Garcia, J. H. Harris, T. C. Hender, B. F. Masden, Phys. Fluids (to be published).

[40] Numerical Algorithms Group USA, Inc., 1131 Warren Ave., Downers Grove, IL 60515.

FIGURE CAPTIONS

Fig. 1. Overall flowchart for AXE.

Fig. 2. Convergence of the Jacobian equation is extremely rapid when enough components are included.

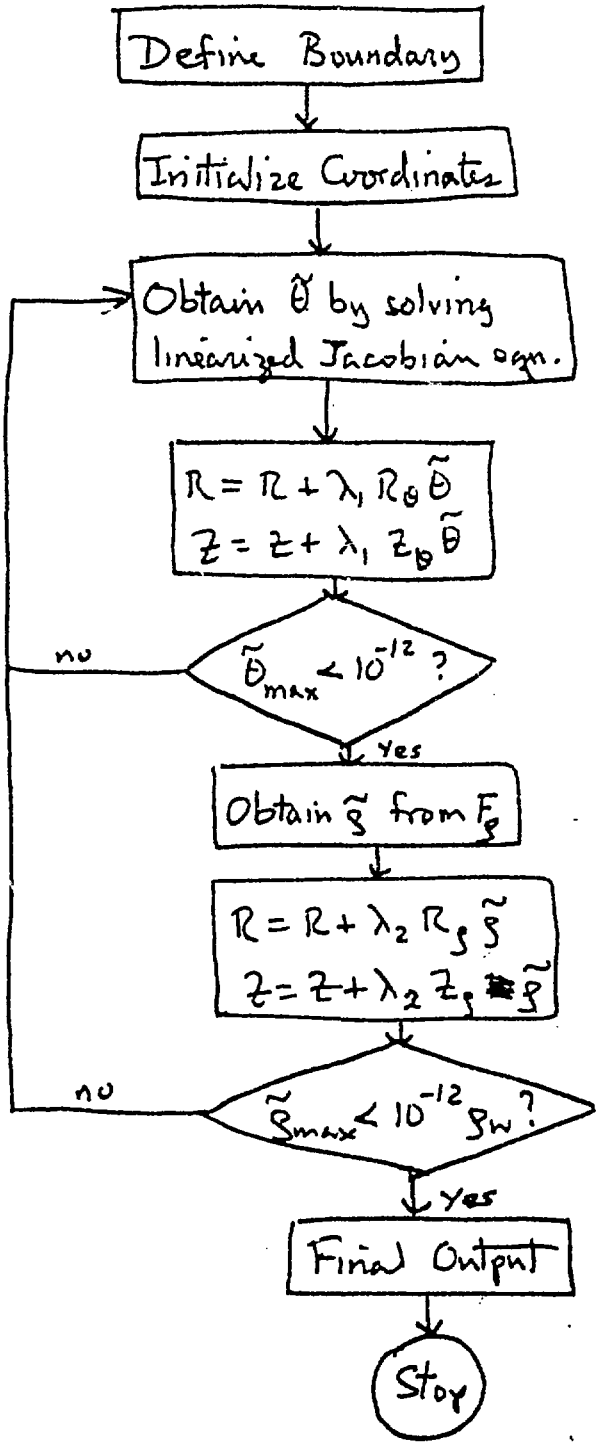
Define Boundary
Initialize Coordinates
Obtain $\tilde{\theta}$ by solving linearized Jacobian eqn.
$R = R + \lambda_1 R_\theta \tilde{\theta}$
$Z = Z + \lambda_1 Z_\theta \tilde{\theta}$
$\tilde{\theta}_{max} < 10^{-12}$?
no
yes
Obtain $\tilde{\xi}$ from F_ξ
$R = R + \lambda_2 R_\xi \tilde{\xi}$
$Z = Z + \lambda_2 Z_\xi \tilde{\xi}$
$\tilde{\xi}_{max} < 10^{-12} \xi_w$?
no
yes
Final Output
Stop

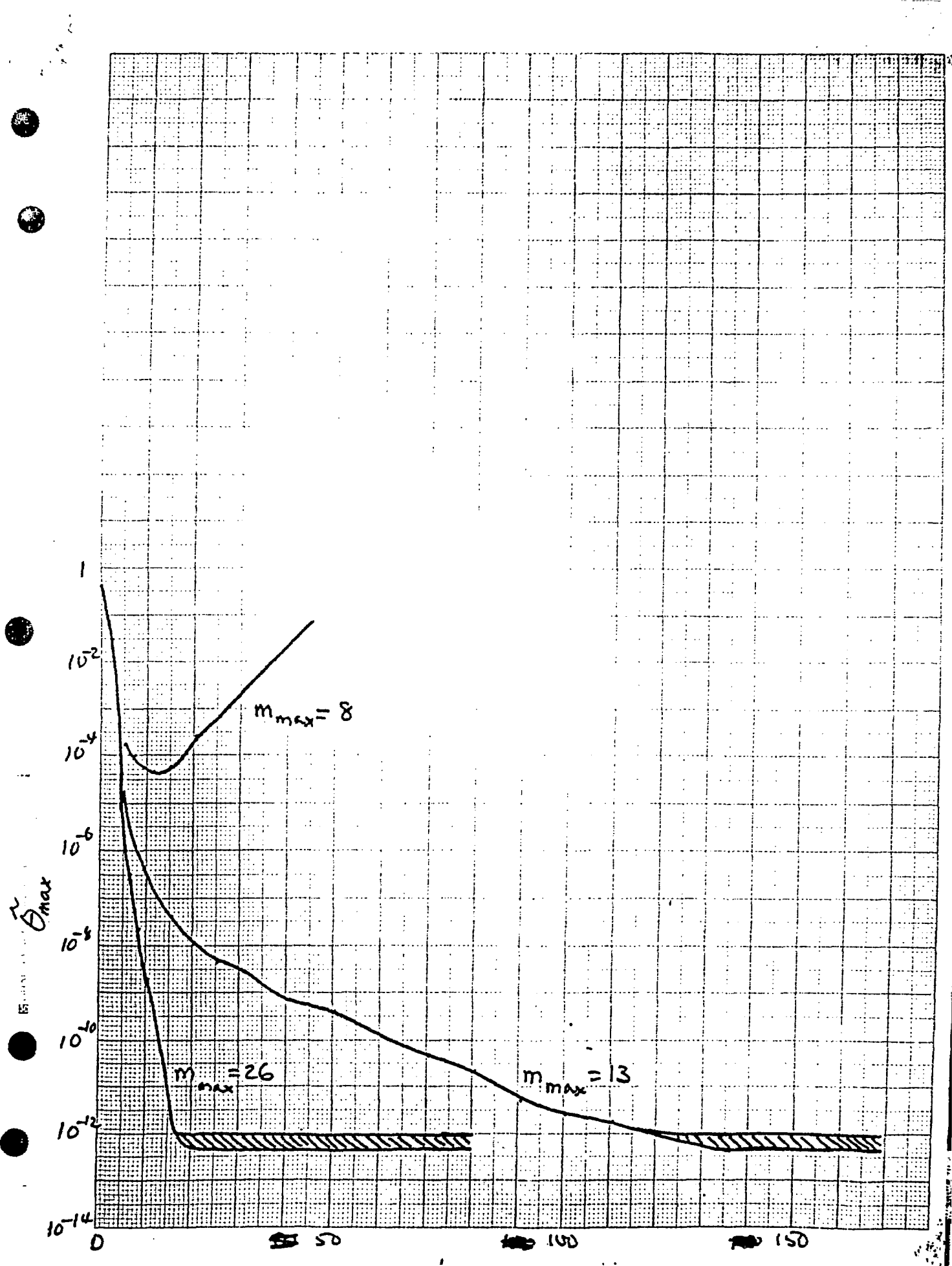
1
10^{-2}
10^{-4}
10^{-6}
10^{-8}
10^{-10}
10^{-12}
10^{-14}
$\tilde{\beta}_{max}$
$m_{max} = 8$
$m_{max} = 26$
$m_{max} = 13$
0
50
100
150

DISCLAIMER